

Deformation Characteristics of Silty Sand Subjected to Water Infiltration

University of Tokyo Member R. P. Orense
 University of Tokyo K. Farooq
 University of Tokyo Member I. Towhata

1. INTRODUCTION

The infiltration of rainwater into an initially unsaturated slope usually results in loss of soil suction, causing a reduction in the available shear strength along the potential failure plane, and eventually leading to slope failure. This process essentially takes place under constant total stress condition, i.e., σ_1 and σ_3 remain unchanged while the pore pressure increases. Figure 1 schematically illustrates the field stress path followed by a soil element under rainwater infiltration conditions. This stress path can be simulated in the laboratory through constant shear drained (CSD) tests.

In this paper, the results of CSD tests on unsaturated silty sand specimens are presented. The effects of various parameters, such as initial relative density (Dr), principal stress ratio ($K = \sigma_1/\sigma_3$) and initial degree of saturation (Sr), on the deformation behavior are discussed.

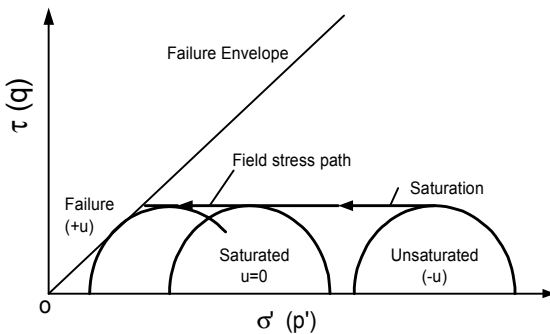


Fig. 1: Field stress path (after Anderson et al. 1995).

2. TEST MATERIAL AND METHOD

The material used in this study is silty sand procured from natural slopes in Kumanodaira, Gunma Prefecture where a series of large-scale landslides occurred in 1950 due to heavy rainfall. The grain size distribution and other physical properties of the test material are shown in Figure 2.

A modified stress-controlled triaxial apparatus was used for the tests. In the tests, the axial and radial deformations were monitored using external linear variable differential

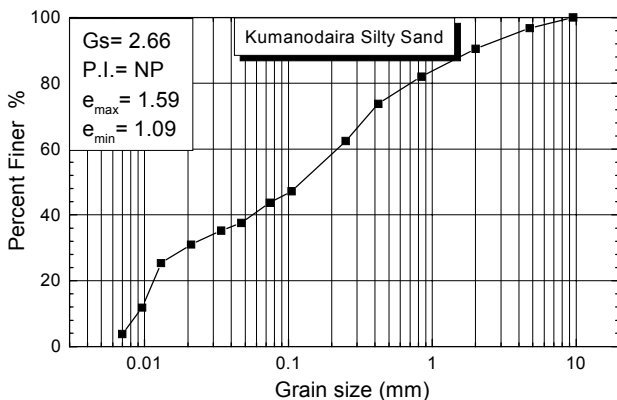


Fig. 2: Grain size distribution of test material.

transducer (LVDT) and clip gages (attached to specimen) respectively. The specimen was 155mm high with a diameter of 75mm. A ceramic disk with air-entry value of 300 kPa was used to measure the initial suction in the specimen. In some of the tests, a miniature pore pressure transducer (PDCR81) was placed inside the specimen to monitor the pore water pressure.

The sample was prepared on top of the saturated ceramic disk by wet tamping method at specified relative density, Dr , and degree of saturation, Sr . After the initial suction stabilized, the specimen was instrumented with deformation transducers. It was first isotropically consolidated and then the axial stress was increased slowly to the specified level of principal stress ratio ($K = \sigma_1/\sigma_3$). After one hour of consolidation, water was infiltrated through the bottom ceramic disk until the specimen failed. During the course of water infiltration, the top cap was vented to atmosphere. The axial load was maintained constant by computer. For test details, refer to Farooq et al. (2002).

3. TEST RESULTS AND DISCUSSION

Figure 3 illustrates the time histories of axial strain (ϵ_a) and over-all degree of saturation (Sr) during the course of water infiltration for specimens under constant $K=2.5$ but with varying Dr (40~80%). The over-all Sr refers to the average value within the specimen. It can be seen that for all cases, the specimens are deforming at constant strain rate $\dot{\epsilon}$ as the Sr continues to increase. After a certain value of Sr is reached, ϵ_a starts to increase suddenly. It can be clearly seen from the figure that the values of overall Sr at the time of failure initiation (shown by Δ) are essentially the same in all the tests, i.e., $Sr \sim 95\%$. In Tests 23 ($Dr=60\%$) and 25 ($Dr=40\%$) where the infiltration rates Q are almost the same, failure starts earlier for denser sample since it has less volume of voids as compared to looser samples. In addition, the effect of Dr on the strain rate after failure initiation, $\dot{\epsilon}$, is evident from the Figure 3, with looser samples undergoing more rapid failure than dense ones.

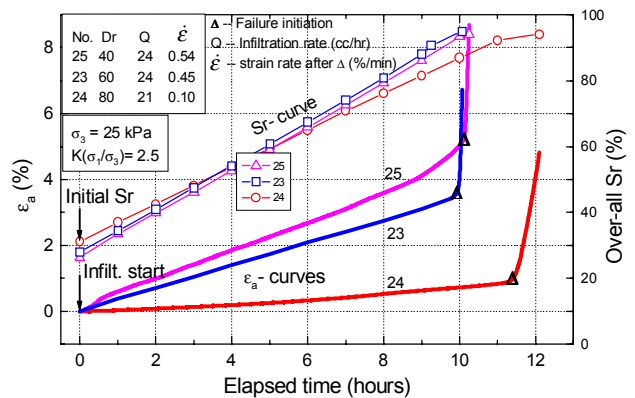


Fig. 3: Effect of Dr on ϵ_a under water infiltration.

Keywords: slope failure, rainfall, unsaturated soil, deformation, stress path, degree of saturation

Dept. of Civil Eng, Univ. of Tokyo, 7-3-1 Hongo, Bunkyo-ku, Tokyo 113-8656 Tel; (03)5841-7452; Fax: (03)5841-8504

Figure 4 shows the test results for specimens with the same Dr but with varying initial K and initial Sr . The effects

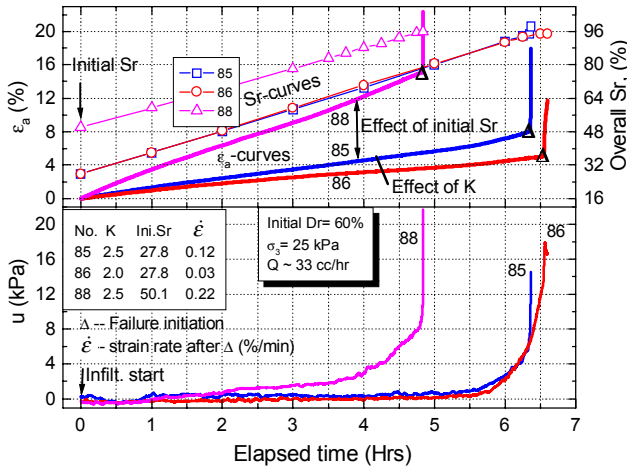


Fig. 4: Effect of K and initial Sr.

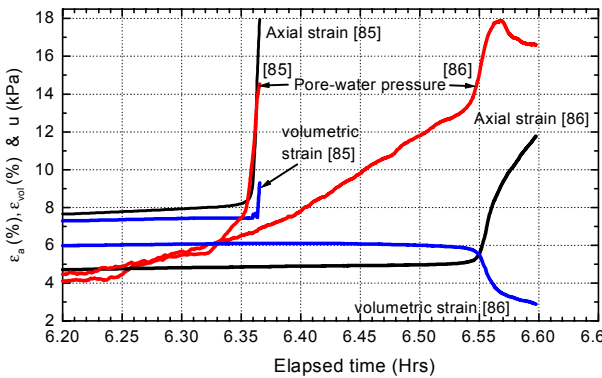


Fig. 5: Conditions near failure (Tests 85 and 86).

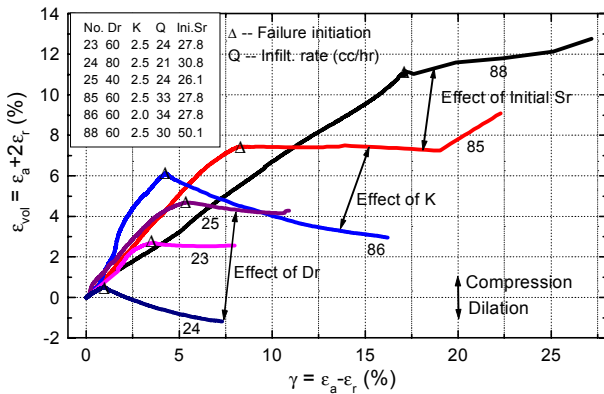


Fig. 6: Volumetric ~ shear strain relations.

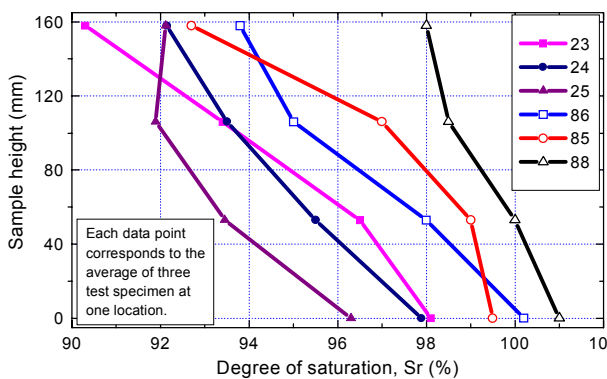


Fig. 7: Variation of actual Sr with sample height.

of K can be seen in Tests 85 ($K=2.5$) and 86 ($K=2.0$) where all other conditions are the same, while the effect of initial Sr was investigated in Tests 85 ($Sr=27.8\%$) and 88 ($Sr=50.1\%$). In these tests, the pore water pressure within the specimen was monitored by installing a miniature pore pressure transducer inside the sample. The upper portion of Figure 4 shows similar pattern as in the earlier case, i.e., almost constant strain rate during water infiltration, followed by rapid development of strain once failure is initiated. It can be seen from the lower portion of the figure that during the initial phase of water infiltration, there is negligible pore water pressure; however, when sufficient Sr is attained, pore water pressure starts developing and consequently, failure is initiated in the specimen. In Test 88 (initial $Sr=50.1\%$), the development of pore water pressure is faster, and consequently, failure is initiated more rapidly.

Figure 5 shows the detailed time histories of axial strain, volumetric strain and pore water pressure for Tests 85 and 86 near the time of failure. From this figure, the dependency of pore water pressure on the shearing mode of the soil after failure initiation is evident. In Test 85, the specimen becomes more contractive when failure is initiated, resulting in rapid increase in pore water pressure leading to a fast failure. In Test 86, on the other hand, the specimen begins to dilate after failure is initiated, resulting in decrease in pore water pressure and consequently, a decline in axial strain rate, $\dot{\epsilon}$, is evident from the figure.

The relations between volumetric strain ϵ_{vol} and shear strain γ are shown in Figure 6. These strain parameters were computed from axial strain ϵ_a and radial strain ϵ_r , as indicated in the figure. It can be seen that prior to initiation of failure, all the specimens show contractive behavior; however, except for Test 88, the behavior becomes dilative once failure is initiated.

Figure 7 shows the variation of actual Sr with the specimen height at the end of each test, obtained by taking small amount of samples at specified locations. It can be seen that in all the tests, the actual Sr is very near full saturation. Moreover, it is worthy to mention that most of the radial deformation occurred in the lower part of the specimen.

Note that the results of pore water pressure measurement are significant when dealing with rainfall-induced slope failures. For soils which undergo contractive behavior, high pore water pressure may developed during the rainwater infiltration and a rapid type of failure can be expected as compared to dilative soils, unless the tendency to lose pore water pressure is compensated by rainwater infiltration.

4. CONCLUDING REMARKS

The main cause of failure initiation is the development of positive pore water pressure. Specimens that exhibited contractive behavior underwent a rapid failure. Initial conditions have profound effect on progress of slope deformation.

REFERENCES

Anderson, S.A. and Sitar, N. 1995. "Analysis of rainfall-induced debris flows," Journal of Geotech. Eng. ASCE, 121, 7, 544-552.

Farooq, K., Orense, R., and Towhata, I. 2002. "Analysis of factors affecting rainfall-induced landslides in sandy slopes," Proc., 3rd Int. Conf. on Unsaturated Soils, 767-772.